Polarization-Dependent Distortion of the Vortex Light Field Generated Using a Vortex Retarder

Jinyu Pan, Zhiyuan Huang, Tiandao Chen, Donghan Liu, Yue Yu, Xinshuo Chang, Meng Pang, and Yuxin Leng

***Abstract*—A vortex retarder (VR) is a widely-used optical component for converting Gaussian light beams into vortex beams, exhibiting unique advantages in a few broadband applications. However, the quality of the vortex beam generated using a VR-based system is highly dependent on the polarization state of the incident light. In this letter, we investigate both theoretically and experimentally the distortion of the output vortex light field resulting from the misalignment of the light polarization state in a VR-based vortex-beam-generation system. While a theoretical model was constructed to study the optical properties of the generated vortex beams at different polarization states of the incident Gaussian beams, systematic characterizations on near- and far-field profiles of the vortex light fields were performed in the experiment. The results exhibit that non-ideal circularly-polarized incident light can introduce a sinusoidal-shape modulation on the optical field, resulting in both phase and intensity distortions of the generated vortex light beam. Our findings provide some insights into the generation and propagation processes of vortex light fields, which could be useful for the practical construction of a VR-based vortex-beam generation system.**

***Index Terms*—Vortex light beam, vortex retarder, polarization state.**

I. Introduction

VORTEX light beams, distinguished by their helical phase fronts and resultant orbital angular momentum (OAM) [1], [2], [3], have gained significant attention in the realm of optics [4], [5], [6], [7]. In addition to the fundamental study of their physical characteristics, such as the coupling of spin and orbital angular momentum [8] and the conservation of OAM in frequency conversion [9], [10], vortex light beams have also found widespread applications in optical telecommunications [11], microscopic manipulation [12], and high-precision fabrication [13]. The continuous expansion of application fields has stimulated developments in the methods of generating vortex light, not only revealing the considerable potential for both basic research and practical applications but also emphasizing the importance of precisely generating and manipulating vortex beams [14], [15]. Certain conditions, such as the lack of uniformity and symmetry in the initial light field, along with the misalignment among optical components, can lead to distortions in both the intensity and phase of the vortex fields. These issues significantly diminish the performance and efficiency of vortex light in practical applications.

The mainstream passive methods for generating vortex light beams include spiral phase plates [16], [17], forked diffraction gratings [18], [19] and Pancharatnam-Berry phase optical elements (PBOEs) [20], etc. Among these, vortex retarders (VRs), as one of the PBOEs, are widely used in various applications due to their significant advantages, including increased insensitivity to chromatic aberration, which is particularly beneficial for scenarios requiring broadband light sources [21], [22]. In VRs, the fast axis orientation is uniformly radial and varies continuously along the azimuthal direction, specifically following the following rule [21], [22]:

$$\phi = \frac{l}{2}\theta \tag{1}$$

where ϕ represents the fast axis orientation, l is the topological charge, and θ is the azimuthal angle. When the incident light is circularly polarized, this arrangement enables the VR to produce vortex light with a helical phase front, thereby imparting OAM to the beam [20]. In practical experiments, achieving a perfectly circularly polarized state is challenging due to factors including imperfections in the polarization elements such as wave plates, and the intrinsic characteristics of the light source itself. The suboptimal circularly polarized state of the incident light is one of the key factors causing distortions in the vortex light fields. However, this aspect of vortex light generation, particularly the influence of the polarization state of the incident light when utilizing VRs to produce vortex light fields has, to the best of our knowledge, not been previously investigated.

In this work, we investigate how the non-ideal circular polarization of the incident light serves as a key factor in causing distortions in the vortex light field. Through theoretical derivation and experimental validation, we demonstrate the relationship between the polarization states of the incident

Manuscript received 7 February 2024; revised 28 February 2024; accepted 2 March 2024. Date of publication 6 March 2024; date of current version 1 April 2024. This work was supported in part by the National Natural Science Foundation of China under Grant 62205353, Grant 62275254, Grant 61925507, and Grant 12388102, in part by the National Postdoctoral Program for Innovative Talents under Grant BX2021328, in part by the China Postdoctoral Science Foundation under Grant 2021M703325, in part by the Zhangjiang Laboratory Construction and Operation Project under Grant 20DZ2210300, in part by the Strategic Priority Research Program of the Chinese Academy of Science under Grant XDB0650000, in part by the Shanghai Science and Technology Plan Project Funding under Grant 23JC1410100, in part by the Shanghai Science and Technology Innovation Action Plan under Grant 21ZR1482700, in part by the National Key R&D Program of China under Grant 2022YFA1604401, and in part by the Shanghai Science and Technology Committee Program under Grant 22DZ1100300, Grant 22560780100, and Grant 23560750200. *(Corresponding authors: Zhiyuan Huang; Meng Pang; Yuxin Leng.)*

Please see the Acknowledgment section of this article for the author affiliations.

Digital Object Identifier 10.1109/JPHOT.2024.3374248

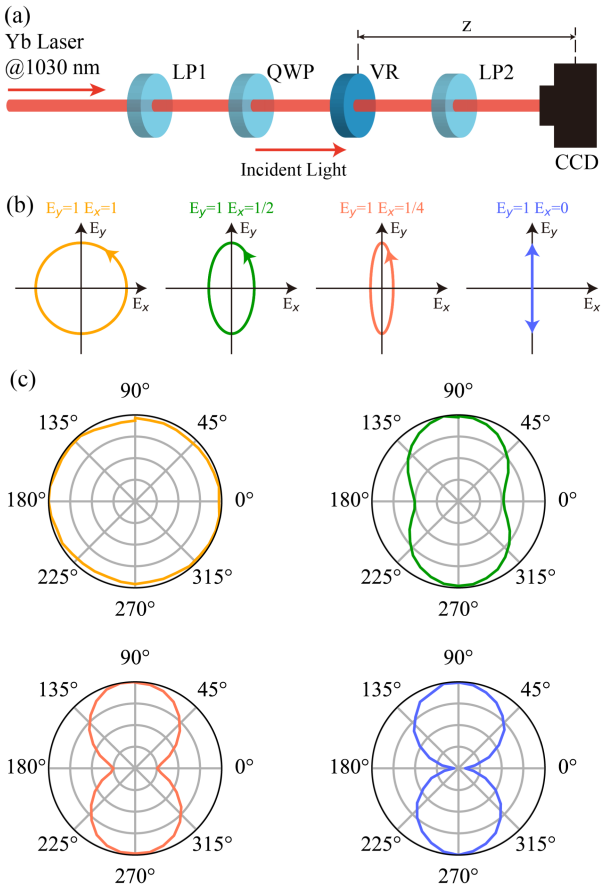

Fig. 1. (a) Schematic of the experimental setup. LP1-LP2, linear polarizer; QWP, quarter-wave plate; VR, vortex retarder. (b) Four distinct polarization states of the incident light set for the experiment. (c) Measured intensity distribution of the electric field for different polarization states before passing through the VR.

light and the resulting spatial characteristics, including the intensity and the phase, of vortex light fields. Our findings reveal that nonideal circular polarization of incident light not only introduces a cosine modulation into the intensity distribution but also affects the phase front of the vortex light field, providing essential knowledge for improving the quality of generated vortex light beams in applications requiring high precision.

II. Experimental Setup and Theoretical Model

The experimental setup used to generate and characterize the vortex light beams under various polarization states of the incident light is shown in Fig. 1(a). The laser beam, generated from an industrial Yb-based laser with an average power of 10 W, first passed through a linear polarizer (LP1) and a quarter-wave plate (QWP) to control the polarization. By setting the fast axis of the QWP in the y direction and finely tuning the LP1 angle, four specific polarization states shown in Fig. 1(b) were achieved, each distinct in the ratio of their major to minor axes: 1:0 for linear, 1:1 for circular, and two elliptical configurations, including 1:1/2 and 1:1/4. These states were characterized by measuring the intensity of various polarization components after the QWP, represented by the polar plots in Fig. 1(c). Subsequently, the beam was directed through a VR that carries a topological charge of 1, followed by another linear polarizer (LP2) oriented in the y direction, resulting in the generation of a linearly polarized vortex light beam. The resulting intensity patterns of the vortex light were ultimately captured by a CCD camera. It should be noted that our experimental design meets the condition for paraxial propagation. In the experiment, we first used two apertures to determine the direction of the optical axis, and then confirmed that the propagation of the beam was aligned with the optical axis. When measuring the intensity of the optical field, we also adjusted the orientation of the CCD camera screen to be perpendicular to the optical axis.

For the theoretical study, we consider an incident light field with Gaussian intensity and elliptical polarization:

$$\vec{E}\ (r,\theta) = \left[E_x\vec{e_x} + E_y \exp\left(\frac{i\pi}{2}\right)\vec{e_y}\right] \exp\left(-\frac{r^2}{w_0^2}\right) \quad (2)$$

where r and θ represent the radial and azimuthal coordinates in the transverse plane, respectively. E_x and E_y are the electric field amplitude components along the x- and y-axes, and w_0 denotes the beam radius, which is set to 1.5 mm in the calculation. The time term is omitted for simplicity because we only focus on spatial characteristics.

Considering the fast axis orientation of the VR, as depicted in (1), the resulting light field after passing through the LP2 is derived as:

$$E_{vy}\ (r,\theta) = \exp\left(-\frac{i\pi}{2}\right)\exp\left(-\frac{r^2}{w_0^2}\right) [(E_y - E_x)\cos(l\theta) + E_x \exp(il\theta)] \quad (3)$$

The light field described by (3) is shown in Fig. 2. The left column shows the intensity distributions for the different polarization states of the incident light, with the colormaps matching the four colors of the corresponding polarization states in Fig. 1(b). When the incident light is perfectly circularly polarized, corresponding to the condition $E_x = E_y$, the intensity of the light field maintains a Gaussian profile. As the misalignment of the principal axis between LP1 and QWP increases, the light intensity distribution after LP2 gradually loses its circular symmetry (see the left column in Fig. 2), meanwhile the phase distribution loses it helical phase structure (see the middle column in Fig. 2). For any state other than linear polarization, the vortex structure is evident in the phase diagrams, which are observable in the middle column of Fig. 2. To delineate the phase variations more clearly, the phase profiles along the beam center, marked by the directional red circles in the middle column, are extracted and presented in the right column. These profiles reveal that only in the case of an ideal circular polarization state does the helical phase structure exhibit a uniform angular gradient. For elliptical polarization states, the phase gradient along the azimuthal direction displays obvious deviation from the ideal helical structure, which exhibits a periodic feature along the azimuthal direction. The periodicity of the deviation has the same pattern as that of the light-intensity distribution,

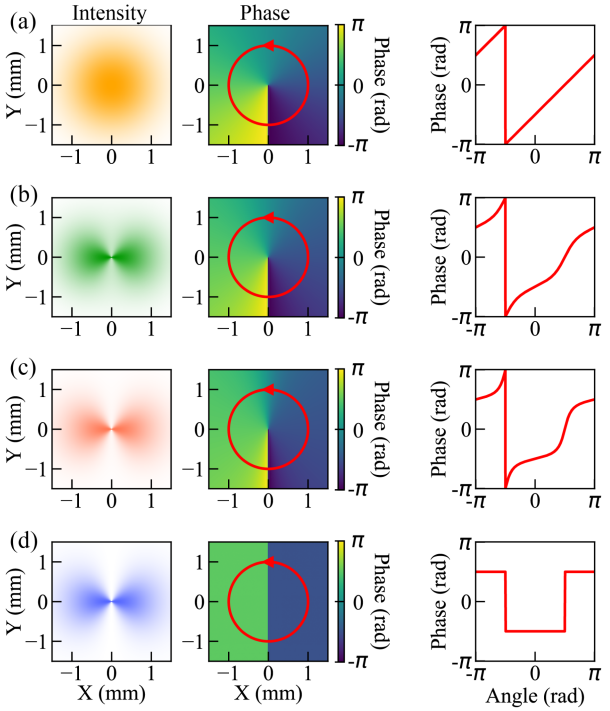

Fig. 2. Simulated intensity distributions and phase profiles of y-polarized components for light fields with different polarization states of the incident light after passing through the VR. (a–d) Each panel corresponds to the polarization states depicted in Fig. 1(b). The left column visualizes the intensity distributions. The middle column depicts the phase profiles. The right column shows the phase profiles extracted along the directional red circles in the phase profiles.

highlighting the close relationship between intensity and phase distortions of the generated light field. Notably, at nearby angles corresponding to the regions of lower intensity, the rate of phase change accelerates, highlighting how elliptically polarized incident light introduces periodic shifts in the phase profile of the vortex beam.

Then we study the influence of this misalignment on the formation of phase singularity in the OAM-carrying light field. We first perform theoretical simulations on the free-space propagation of the light field after LP2. We used (3) as the initial condition in the Collins integral formula and thereby derived the electric field expression at any given propagation distance along the axis [22], [23], [24]:

$$\begin{aligned} E_{vy}\ (r,\theta,z) = &\exp\left(-\frac{i\pi}{2}\right)\frac{(-i)^{|l|+1}k}{z}\exp\left(ikz\right) \\ &\times \exp\left(\frac{ikr^2}{2z}\right)\frac{\sqrt{\pi}b}{8\sqrt{a^3}}\exp\left(-\frac{b^2}{8a}\right) \\ &\left[I_{\frac{|l|-1}{2}}\left(\frac{b^2}{8a}\right) - I_{\frac{|l|+1}{2}}\left(\frac{b^2}{8a}\right)\right] \\ &\times \left[(E_y - E_x)\cos\left(l\theta\right) + E_x\exp\left(il\theta\right)\right] \end{aligned} \quad (4)$$

where k is the wavenumber of the light, z is the propagation distance, $I_n(\cdot)$ is the modified Bessel function of the first kind, a and b are coefficients related to the Gaussian beam parameters and the propagation distance:

$$a = \frac{1}{w_0^2} - \frac{ik}{2z} \quad (5)$$

$$b = \frac{kr}{z} \quad (6)$$

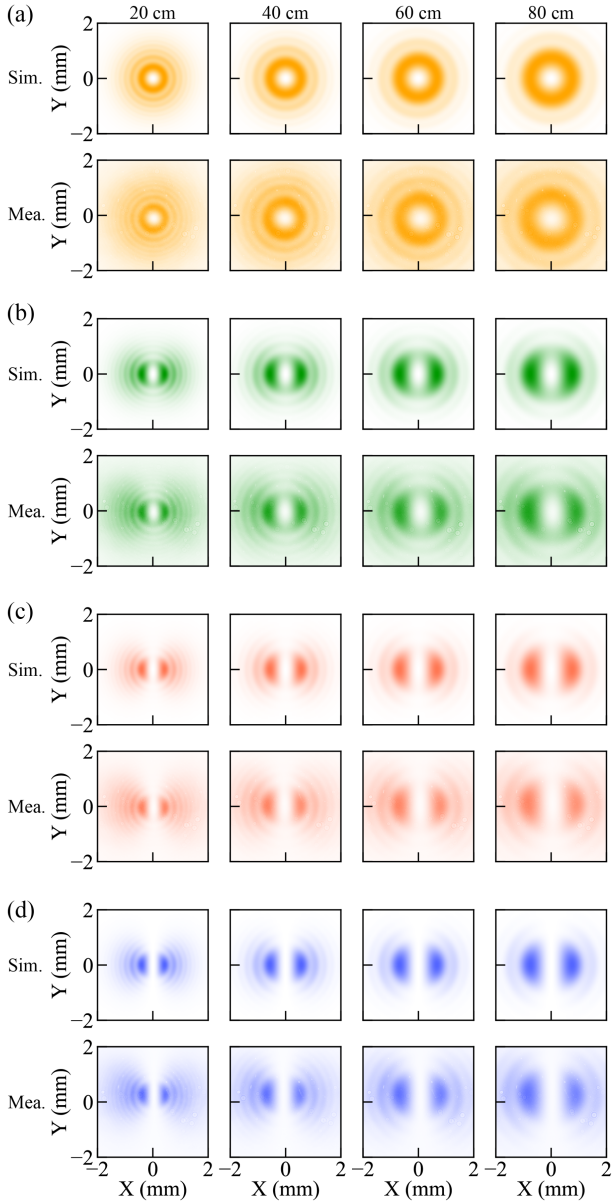

Fig. 3. Simulated and measured intensity distributions under different polarization states of the incident light at the propagation distances of 20 cm, 40 cm, 60 cm, and 80 cm. (a–d) Each panel corresponds to one of the polarization states depicted in Fig. 1(b).

III. Results and Analysis

Following the theoretical formulation outlined in (4), we proceeded to validate our model by examining the intensity distribution of the light field under varying polarization states of the incident light. Fig. 3 illustrates these intensity distributions at the propagation distances of 20 cm, 40 cm, 60 cm, and 80 cm.

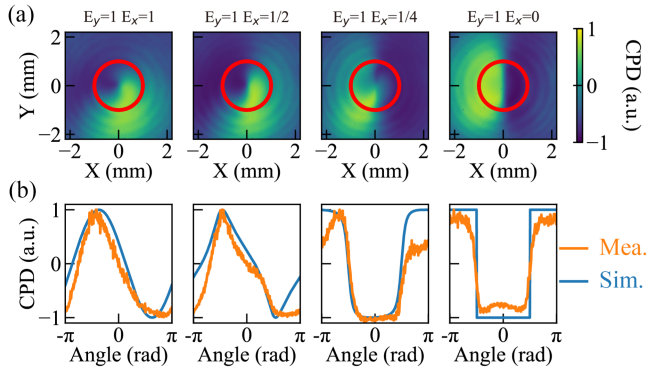

Fig. 4. (a) CPD patterns for the different polarization states of the incident light. (b) Extracted CPD along the red circle in (a) (orange line) and simulated CPD at the same position (blue line).

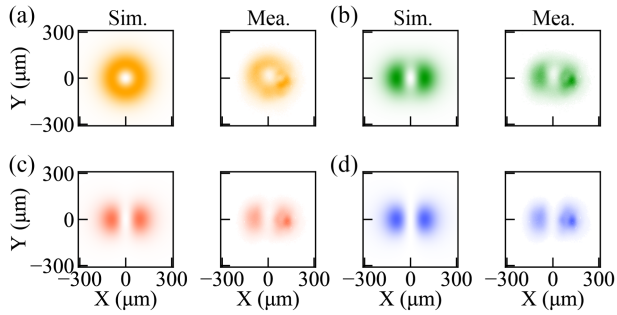

Fig. 5. Simulated and measured focal field distributions for different polarization states of the incident light depicted in Fig. 1(b).

Each panel corresponds to the polarization state depicted using the same color in Fig. 1(b). The upper rows display the simulated intensity profiles derived from our theoretical model, while the lower rows show the corresponding experimental measurements captured by a CCD camera placed at specified distances from the VR, as described in Fig. 1(a). The good consistency between the theoretical simulations and the experimental results demonstrates the accuracy of our electric field expression in predicting the behavior of light fields.

As the polarization state of the incident light deviates from the ideal circular condition ($E_x = E_y$), the intensity distribution begins to exhibit a cosine modulation, as indicated by the alternating bright and dark regions. With increasing ellipticity of the polarization state, not only does this modulation become more pronounced but also the morphology of the central dark region is affected. For ideally circularly polarized incident light, this dark region appears as a uniform circle. However, deviations from this ideal state result in a gradual distortion of this central dark region, morphing from a circular to a more elongated, rectangular form. Significantly, the size of the dark region increases with propagation distance, indicating a spread in the vortex beam's phase singularity.

Fig. 4 demonstrates the phase distortion induced by the non-ideal polarization states of the incident light through an interference experiment. Here, a reference beam, which was split from the beam by a beam splitter before LP1, was made to interfere with the vortex beam. The interference patterns were captured by a CCD camera at the position of z = 60 cm. The cosine of the phase difference (CPD) between the two beams can be extracted from the interference patterns, which can be expressed as:

$$CPD = \frac{I_I - I_V - I_R}{A\sqrt{I_V I_R}} \tag{7}$$

where I_I is the intensity of the interference patterns, I_V and I_R are the intensity of the vortex beam and the reference beam, respectively. A is a constant related to the delay between the two beams.

In Fig. 4(a), we observe the CPD patterns for the different polarization states of the incident light. Fig. 4(b) shows the extracted CPD along the red circle in Fig. 4(a), providing a direct comparison between the experimental results and theoretical simulations. The plots reveal the transformation of the CPD as the polarization state varies from circular to linear, with the experimental curves closely following the theoretical predictions. The deviation from the ideal circular polarization manifests as a clear modulation in the CPD, confirming the influence of the polarization state of the incident light on the phase property of the vortex beam.

Furthermore, we investigated the focal spot generated by vortex light beams under various polarization states of the incident light. In the experiment, a lens with a focal length of 500 mm was positioned 20 cm away from the VR (z = 20 cm) along the propagation direction of the light, and the focal spot was captured using a CCD camera. In the simulations, we first applied (4) with z set to 20 cm to calculate the light field distribution at the position of the lens. We then performed a two-dimensional Fourier transform on this calculated light field to theoretically predict the focal spot morphology [25]. Fig. 5 shows the experimental and theoretical results for the focal spots. The observed nonuniformities in the measured focal spots may be attributed to imperfections in the optical path, such as flawed components or inhomogeneities in the manufacturing of the devices, which could introduce phase disturbances to the light field. The influence of the incident light polarization state on the focal spot morphology is similar to its impact on the light field profile during free space propagation. While the central features and asymmetries imposed by the polarization state remain prominent, the diffraction rings observed in free propagation are absent at the focus.

IV. Conclusion

In conclusion, our investigation reveals the impact of the polarization state of incident light on vortex light field generation using VRs. We observed that nonideal circular polarization of the incident light introduces a cosine modulation into the intensity of the light field, primarily morphing the central dark region and altering the structure of the phase front. The focal spot is also affected by this modulation, demonstrating a nuanced dependence on the polarization state of the incident light. The results underscore the intricate behavior of vortex light fields under various polarization states of incident light and emphasize

the need for precise control in applications using structured light. The insights gained in our work pave the way for further exploration in customizing light-matter interactions using vortex beams.

Acknowledgment

Authors' Affiliations

Jinyu Pan, Yue Yu, and Xinshuo Chang are with the State Key Laboratory of High Field Laser Physics and CAS Center for Excellence in Ultraintense Laser Science, Shanghai Institute of Optics and Fine Mechanics (SIOM), Chinese Academy of Sciences (CAS), Shanghai 201800, China, also with the Hangzhou Institute for Advanced Study, Chinese Academy of Sciences, Hangzhou 310024, China, and also with the Center of Materials Science and Optoelectronics Engineering, University of Chinese Academy of Sciences, Beijing 100049, China.

Zhiyuan Huang is with the State Key Laboratory of High Field Laser Physics and CAS Center for Excellence in Ultraintense Laser Science, Shanghai Institute of Optics and Fine Mechanics (SIOM), Chinese Academy of Sciences (CAS), Shanghai 201800, China, and also with the Russell Centre for Advanced Lightwave Science, Shanghai Institute of Optics and Fine Mechanics and Hangzhou Institute of Optics and Fine Mechanics, Hangzhou 311421, China (e-mail: huangzhiyuan@siom.ac.cn).

Tiandao Chen is with the State Key Laboratory of High Field Laser Physics and CAS Center for Excellence in Ultraintense Laser Science, Shanghai Institute of Optics and Fine Mechanics (SIOM), Chinese Academy of Sciences (CAS), Shanghai 201800, China, and also with the Center of Materials Science and Optoelectronics Engineering, University of Chinese Academy of Sciences, Beijing 100049, China.

Donghan Liu is with the State Key Laboratory of High Field Laser Physics and CAS Center for Excellence in Ultraintense Laser Science, Shanghai Institute of Optics and Fine Mechanics (SIOM), Chinese Academy of Sciences (CAS), Shanghai 201800, China, also with the Russell Centre for Advanced Lightwave Science, Shanghai Institute of Optics and Fine Mechanics and Hangzhou Institute of Optics and Fine Mechanics, Hangzhou 311421, China, and also with the Center of Materials Science and Optoelectronics Engineering, University of Chinese Academy of Sciences, Beijing 100049, China.

Meng Pang is with the State Key Laboratory of High Field Laser Physics and CAS Center for Excellence in Ultraintense Laser Science, Shanghai Institute of Optics and Fine Mechanics (SIOM), Chinese Academy of Sciences (CAS), Shanghai 201800, China, also with the Russell Centre for Advanced Lightwave Science, Shanghai Institute of Optics and Fine Mechanics and Hangzhou Institute of Optics and Fine Mechanics, Hangzhou 311421, China, and also with the Hangzhou Institute for Advanced Study, Chinese Academy of Sciences, Hangzhou 310024, China (e-mail: pangmeng@siom.ac.cn).

Yuxin Leng is with the State Key Laboratory of High Field Laser Physics and CAS Center for Excellence in Ultraintense Laser Science, Shanghai Institute of Optics and Fine Mechanics (SIOM), Chinese Academy of Sciences (CAS), Shanghai 201800, China, and also with the Hangzhou Institute for Advanced Study, Chinese Academy of Sciences, Hangzhou 310024, China (e-mail: lengyuxin@siom.ac.cn).

References

[1] P. Coullet, L. Gil, and F. Rocca, "Optical vortices," *Opt. Commun.*, vol. 73, pp. 403–408, 1989.

[2] L. Allen, M. W. Beijersbergen, R. J. C. Spreeuw, and J. P. Woerdman, "Orbital angular momentum of light and the transformation of Laguerre-Gaussian laser modes," *Phys. Rev. A*, vol. 45, pp. 8185–8189, 1992.

[3] A. Chong, C. Wan, J. Chen, and Q. Zhan, "Generation of spatiotemporal optical vortices with controllable transverse orbital angular momentum," *Nature Photon.*, vol. 14, pp. 350–354, 2020.

[4] A. M. Yao and M. J. Padgett, "Orbital angular momentum: Origins, behavior and applications," *Adv. Opt. Photon.*, vol. 3, pp. 161–204, 2011.

[5] S. Ramachandran and P. Kristensen, "Optical vortices in fiber," *Nanophotonics*, vol. 2, pp. 455–474, 2013.

[6] Y. Shen et al., "Optical vortices 30 years on: OAM manipulation from topological charge to multiple singularities," *Light Sci. Appl.*, vol. 8, 2019, Art. no. 90.

[7] H. Wang et al., "Recent advances in generation of terahertz vortex beams and their applications," *Chin. Phys. B*, vol. 29, 2020, Art. no. 097404.

[8] Y. Zhao, J. S. Edgar, G. D. M. Jeffries, D. McGloin, and D. T. Chiu, "Spin-to-orbital angular momentum conversion in a strongly focused optical beam," *Phys. Rev. Lett.*, vol. 99, 2007, Art. no. 073901.

[9] R. Ni, Y. F. Niu, L. Du, X. P. Hu, Y. Zhang, and S. N. Zhu, "Topological charge transfer in frequency doubling of fractional orbital angular momentum state," *Appl. Phys. Lett.*, vol. 109, 2016, Art. no. 151103.

[10] X. Fang et al., "Examining second-harmonic generation of high-order Laguerre–Gaussian modes through a single cylindrical lens," *Opt. Lett.*, vol. 42, pp. 4387–4390, 2017.

[11] N. Bozinovic et al., "Terabit-scale orbital angular momentum mode division multiplexing in fibers," *Science*, vol. 340, pp. 1545–1548, 2013.

[12] M. Padgett and R. Bowman, "Tweezers with a twist," *Nature Photon.*, vol. 5, pp. 343–348, 2011.

[13] G. Knöner, S. Parkin, T. A. Nieminen, V. L. Y. Loke, N. R. Heckenberg, and H. Rubinsztein-Dunlop, "Integrated optomechanical microelements," *Opt. Exp.*, vol. 15, pp. 5521–5530, 2007.

[14] R. Barboza, U. Bortolozzo, M. G. Clerc, S. Residori, and E. Vidal-Henriquez, "Optical vortex induction via light–matter interaction in liquid-crystal media," *Adv. Opt. Photon.*, vol. 7, pp. 635–683, 2015.

[15] X. Wang, Z. Nie, Y. Liang, J. Wang, T. Li, and B. Jia, "Recent advances on optical vortex generation," *Nanophotonics*, vol. 7, pp. 1533–1556, 2018.

[16] S. N. Khonina, V. V. Kotlyar, M. V. Shinkaryev, V. A. Soifer, and G. V. Uspleniev, "The phase rotor filter," *J. Modern Opt.*, vol. 39, pp. 1147–1154, 1992.

[17] M. Miranda et al., "Spatiotemporal characterization of ultrashort optical vortex pulses," *J. Modern Opt.*, vol. 64, pp. S1–S6, 2017.

[18] V. Y. Bazhenov, M. V. Vasnetsov, and M. S. Soskin, "Laser beams with screw dislocations in their wavefronts," *JEPT Lett.*, vol. 52, pp. 429–431, 1990.

[19] N. R. Heckenberg, R. McDuff, C. P. Smith, H. Rubinsztein-Dunlop, and M. J. Wegener, "Laser beams with phase singularities," *Opt. Quantum Electron.*, vol. 24, pp. S951–S962, 1992.

[20] L. Marrucci, C. Manzo, and D. Paparo, "Pancharatnam-Berry phase optical elements for wave front shaping in the visible domain: Switchable helical mode generation," *Appl. Phys. Lett.*, vol. 88, 2006, Art. no. 221102.

[21] T. Tapani, H. Lin, A. De Andres, S. W. Jolly, H. Bhuvanendran, and N. Maccaferri, "Vortex plate retarder-based approach for the generation of sub-20 fs light pulses carrying orbital angular momentum," *J. Opt.*, vol. 26, 2024, Art. no. 045502.

[22] J. Pan et al., "Self-referencing 3D characterization of ultrafast optical-vortex beams using tilted interference TERMITES technique," *Laser Photon. Rev.*, vol. 17, 2023, Art. no. 2200697.

[23] J. Wen, L. Wang, X. Yang, J. Zhang, and S. Zhu, "Vortex strength and beam propagation factor of fractional vortex beams," *Opt. Exp.*, vol. 27, pp. 5893–5904, 2019.

[24] V. V. Kotlyar, A. A. Almazov, S. N. Khonina, V. A. Soifer, H. Elfstrom, and J. Turunen, "Generation of phase singularity through diffracting a plane or Gaussian beam by a spiral phase plate," *J. Opt. Soc. Amer. A*, vol. 22, pp. 849–861, 2005.

[25] G. Pariente, V. Gallet, A. Borot, and F. Quéré, "Space–time characterization of ultra-intense femtosecond laser beams," *Nature Photon.*, vol. 10, pp. 547–553, 2016.